JCTC Journal of Chemical Theory and Computation

Article

pubs.acs.org/JCTC

Construction and Application of a New Dual-Hybrid Random Phase Approximation

Pál D. Mezei,[*,†] Gábor I. Csonka,[*,†] Adrienn Ruzsinszky,[‡] and Mihály Kállay[§]

[†]Department of Inorganic and Analytical Chemistry, Budapest University of Technology and Economics, H-1521 Budapest, Hungary

[‡]Department of Physics, Temple University, Philadelphia, Pennsylvania 19122, United States

[§]MTA-BME Lendület Quantum Chemistry Research Group, Department of Physical Chemistry and Materials Science, Budapest University of Technology and Economics, P.O. Box 91, H-1521 Budapest, Hungary

Supporting Information

ABSTRACT: The direct random phase approximation (dRPA) combined with Kohn–Sham reference orbitals is among the most promising tools in computational chemistry and applicable in many areas of chemistry and physics. The reason for this is that it scales as N^4 with the system size, which is a considerable advantage over the accurate ab initio wave function methods like standard coupled-cluster. dRPA also yields a considerably more accurate description of thermodynamic and electronic properties than standard density-functional theory methods. It is also able to describe strong static electron correlation effects even in large systems with a small or vanishing band gap missed by common single-reference methods. However, dRPA has several flaws due to its self-correlation error. In order to obtain accurate and precise reaction energies, barriers and noncovalent intra- and intermolecular interactions, we construct a new dual-hybrid dRPA (hybridization of exact and semilocal exchange in both the energy and the orbitals) and test the performance of this new functional on isogyric, isodesmic, hypohomodesmotic, homodesmotic, and hyperhomodesmotic reaction classes. We also use a test set of 14 Diels–Alder reactions, six atomization energies (AE6), 38 hydrocarbon atomization energies, and 100 reaction barrier heights (DBH24, HT-BH38, and NHT-BH38). For noncovalent complexes, we use the NCCE31 and S22 test sets. To test the intramolecular interactions, we use a set of alkane, cysteine, phenylalanine-glycine-glycine tripeptide, and monosaccharide conformers. We also discuss the delocalization and static correlation errors. We show that a universally accurate description of chemical properties can be provided by a large, 75% exact exchange mixing both in the calculation of the reference orbitals and the final energy.

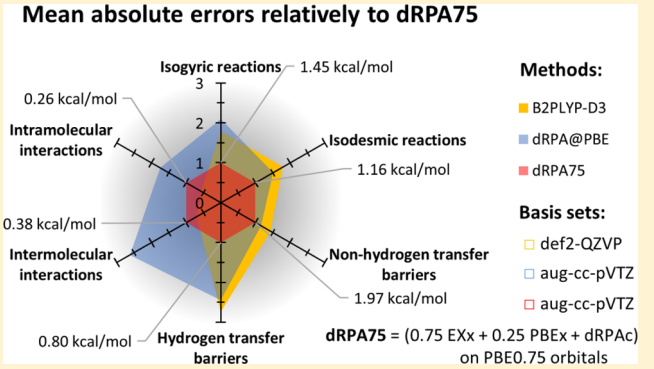

INTRODUCTION

Within the direct Random Phase Approximation (dRPA)[1−6] framework, the addition of the exact exchange (EX) and the dRPA correlation (dRPAc) results in an orbital dependent functional, which has many desirable features. dRPAc can be constructed either in the framework of density functional theory or in the ring coupled cluster formalism.[7] The fully nonlocal dRPAc seamlessly integrates dispersion interactions, the EX is free of self-interaction error (SIE), and dRPA is applicable to small-gap or metallic systems because the "ring" diagrams are summed to infinite order. dRPA is accurate for intra- and intermolecular noncovalent interactions,[8,9] for adsorption,[10,11] for interlayer interactions,[12] and for van der Waals bonded solids.[13] However, the method has several serious disadvantages because the dRPAc energy is spoiled by the self-correlation error, the total energies are systematically and significantly overestimated in magnitude as the dRPAc overestimates the correlation at short-range.[1,14,15] Consequently, dRPA fails seriously in the description of changes which lead to short-range rearrangement of the electronic structure.[2] RPA performs moderately for covalent bond breaking reaction energies,[7] and it underestimates the binding energies. RPA overestimates the ionization potentials[16] and underestimates the atomization energies of molecules[17] and solids.[18]

There is also no practical self-consistent dRPA implementation in the adiabatic-connection fluctuation–dissipation theorem (ACDFT) density functional approach. The nonself-consistent results are written in the form of method@orbitals in the literature such as dRPA@DFT or (EX + dRPAc)@DFT.[19] Practical (EX + dRPAc)@DFT calculations are commonly performed in a postprocessing way, where single-particle orbitals from a self-consistent DFT calculation are used to evaluate both the EX and dRPAc terms. In this paper, the mean deviation from the reference energies is abbreviated as MD, and

Received: May 7, 2015

DOI: 10.1021/acs.jctc.5b00420
J. Chem. Theory Comput. XXXX, XXX, XXX−XXX

the mean absolute deviation from the reference energies is abbreviated as MAD. Paier et al. reported[20] that (EX + dRPAc)@PBE provides accurate results for the barrier heights of the hydrogen transfer reactions in the HT-BH38 database[21] (MD = −0.2 kcal mol^{-1}, MAD = 1.7 kcal mol^{-1}) but significantly underestimates the barrier heights of heavy atom, non-hydrogen transfer (NHT) reactions in the NHT-BH38 database (MD = −2.51 kcal mol^{-1}, MAD = 2.89 kcal mol^{-1}) compared to the moderately accurate W1 level reference energies. Only modest improvements using the corrected (EX + dRPAc + SOSEX + rSE)@PBE were achieved for HT reaction barriers, where SOSEX stands for Second-Order Screened Exchange,[22] and rSE refers to renormalized single excitations within the Rayleigh−Schrödinger perturbation theory.[19] The NHT reaction barriers are even worsened due to the SOSEX and rSE corrections.[20] The SOSEX correction to dRPA about halves the large underbinding atomization error of dRPA.[23] Adding rSE correction to dRPA + SOSEX improves further the atomization energies.[20] Notice also that dRPA + SOSEX is one-electron self-correlation free.[24] Ren et al. suggested[19] replacing the EX@PBE reference energy with the HF total energy. This HF + (dRPAc)@PBE hybrid method (dRPAh) improves binding energies of molecules and solids by almost 50% compared to (EX + dRPAc)@PBE.

Sai et al. observed[25] that a large fraction of exact exchange in the PBE hybrid can eliminate the consequences of the many-electron SIE. To achieve many-electron SIE-freedom, the ground state total energy $E(N)$ should be linear in the electron number N between integers and should have a realistic slope.[26−29] This condition was achieved for benzene, naphthalene, and anthracene by mixing 0.7 fraction of exact exchange with 0.3 fraction of PBE exchange in a PBE hybrid.[25] This hybrid gives an accurate description for ionization and dimer dissociation.[25] The predicted formation energies of both localized and delocalized holes in perfect molecular crystals due to ionization are consistent with experimental values.[25]

Atalla et al. proposed[30] a scheme to obtain an unambiguous system-dependent fraction of exact exchange for hybrid DFT that is consistent with the G0W0 approach, where G0 is the noninteracting Green's function of the system and W0 is the screened Coulomb interaction. To achieve this the exact condition of DFT was used: the energy of the highest occupied molecular orbital corresponds to the ionization potential.[31] The approach which uses 0.8 fraction of exact exchange is essential for describing electron transfer in the TTF/TCNQ dimer and yields the vertical ionization potentials of the G2 test set with a mean absolute percentage error of only ≈3%.

Macher et al. compared[32] the performance of the (EX + dRPAc)@PBE and the hybrid HF + (dRPAc)@PBE for ice. The (EX + dRPAc)@PBE underestimates the binding energies and overestimates all predicted volumes. The HF + (dRPAc)@PBE overestimates the binding energy and underestimates the equilibrium volumes. A simple solution for this problem suggested by Macher et al. is to determine the exact exchange energy from orbitals of a functional in which half of the HF exchange is mixed with half of the DFT exchange.

Heßelmann proposed the RPAX2 method based on PBE exchange (PBEx) reference orbitals.[33] RPAX2 is obtained by a simple modification of the ring coupled-cluster doubles amplitude equation and by a slightly modified update equation for the amplitudes. Numerical tests for chemical reaction energies and intermolecular interaction energies have shown that the RPAX2 method, if it is based on a PBEx Kohn−Sham reference determinant, yields results which are very close to coupled-cluster with single, double, and perturbative triple excitations (CCSD(T)) reference results.

Using the renormalized perturbation theory, Bates and Furche developed a promising beyond-RPA approximate exchange kernel (AXK) method.[34] AXK yields a significant improvement for atomization energies and ionization potentials compared to dRPA without affecting reaction barriers. AXK improves the binding energy of H_2 compared to SOSEX but reintroduces some self-interaction error in the binding energy curve of H_2^+.

In this paper, the exact exchange and dRPA correlation energies are calculated based on self-consistent HF, PBE, or PBE hybrid orbitals. We develop a new dual-hybrid dRPA functional and test it on test sets for chemical reaction energies, atomization energies, barrier heights (not involving the zero-point vibration energies), intermolecular weak interactions, and intramolecular noncovalent interactions. We use high level reference energies up to CCSDT(Q)/CBS and compare the performance of the new dual-hybrid functional to the performance of dRPA based on HF and DFT determinants, RPAX2 and double hybrid methods. We use MD as a measure of the accuracy and the corrected sample standard deviation ($CSSD = ((\sum_{i=1}^{N}(x_i - \bar{x})^2)/(N-1))^{1/2}$, where N is the number of elements in the sample) as a measure of the precision. Notice that a small MAD signals that a method is accurate and precise at the same time, but larger MAD above 1−2 kcal mol^{-1} does not always characterize sufficiently the problem with a method (e.g., underbinding or overbinding, etc.).

METHODOLOGY

In the semilocal (*sl*) global hybrid (*gh*) density functional theory, the exchange-correlation energy, E_{XC}^{gh}, is given by mixing the *sl* exchange, E_X^{sl}, with the exact exchange energy, E_X^{exact}, and adding a *sl* correlation energy, E_C^{sl}

$$E_{XC}^{gh} = aE_X^{exact} + (1-a)E_X^{sl} + E_C^{sl} \quad (1)$$

where a is the mixing factor.

In a global double hybrid (*gdh*) functional, the correlation energy is expressed by mixing the semilocal correlation energy with the second-order perturbation theory correlation energy, E_C^{PT2}, calculated on the Kohn−Sham (KS) orbitals.

$$E_{XC}^{gdh} = a_X E_X^{exact} + (1-a_X)E_X^{sl} + a_C E_C^{PT2} + (1-a_C)E_C^{sl} \quad (2)$$

These functionals perform well for molecules but suffer from problems like MP2 as they overestimate the binding energy of systems with small HOMO−LUMO energy gaps. Here we examine three popular functionals based on PT2 (B2PLYP),[35] spin-component scaled PT2 (DSD-BLYP),[36] and scaled opposite spin PT2 (PWPB95).[37]

The direct random phase approximation (dRPA) exchange-correlation energy is given by eq 2

$$E_{XC}^{dRPA} = E_X^{exact} + E_C^{dRPA} \quad (3)$$

where the dRPA correlation energy is given by the following equation

$$E_C^{dRPA} = \frac{1}{2}\mathrm{tr}[\boldsymbol{BT}] \quad (4)$$

where $\boldsymbol{B}$ is the nonantisymmetrized two-electron repulsion integral matrix defined by the $B_{ia,jb} = \langle ijlab\rangle$ four-index matrix

DOI: 10.1021/acs.jctc.5b00420
J. Chem. Theory Comput. XXXX, XXX, XXX−XXX

elements, and $\boldsymbol{T}$ is the double excitation amplitude matrix given by the iterative procedure (initialized with $\boldsymbol{T}^{(0)} = \boldsymbol{0}$) as a Hadamard product with $\boldsymbol{\Delta}$:

$$\boldsymbol{T}^{(n+1)} = -\boldsymbol{\Delta}\circ(\boldsymbol{B} + \boldsymbol{B}\boldsymbol{T}^{(n)} + \boldsymbol{T}^{(n)}\boldsymbol{B} + \boldsymbol{T}^{(n)}\boldsymbol{B}\boldsymbol{T}^{(n)}) \quad (5)$$

The $\boldsymbol{\Delta}$ matrix is defined by the $\Delta_{ia,jb} = 1/(\epsilon_a + \epsilon_b - \epsilon_i - \epsilon_j)$ matrix elements. The equations are solved in an $O(N^4)$-scaling iterative procedure by density-fitted form of electron repulsion integrals and Cholesky decomposition of the orbital energy denominators $\boldsymbol{\Delta}$.[3338] For small HOMO−LUMO gap (e.g., metallic) systems a plasmon-formula-based algorithm is executed in order to prevent unphysical solution or divergence as described in ref 38.

The RPAX2 correlation energy is defined by eq 6, where we suppose that $\boldsymbol{B}$ is written in density-fitted form as $\boldsymbol{B} = \boldsymbol{L}\,\boldsymbol{L}^T$.

$$E_C^{\mathrm{RPAX2}} = \frac{1}{2}\mathrm{tr}[\boldsymbol{L}^T\boldsymbol{T}^{(\infty)}\boldsymbol{L}] \quad (6)$$

The iteration is initialized with $\boldsymbol{T}^{(0)} = \boldsymbol{0}$, then the amplitudes of the iteration cycles are given by

$$\boldsymbol{T}^{(n+1)} = -\boldsymbol{\Delta}\circ[(\boldsymbol{1} + \boldsymbol{T}^{(n)})\boldsymbol{B}(\boldsymbol{1} + \boldsymbol{T}^{(n)}) - \hat{P}(\boldsymbol{1} + \boldsymbol{T}^{(n)})\boldsymbol{B}(\boldsymbol{1} + \boldsymbol{T}^{(n)})] \quad (7)$$

where $\hat{P}$ is a permutation operator that permutes the orbitals. $\boldsymbol{\Delta}$ is decomposed using the Cholesky decomposition. The equations are solved in an $O(N^5)$-scaling iterative procedure.

RPA correlation energy can be calculated with self-consistent DFT or HF calculations, and we also use reference orbitals from self-consistent hybrid DFT calculations. In this work, we propose a scheme of hybrid (eq 8) and double hybrid (eq 9) dRPA energies evaluated using reference orbitals from self-consistent hybrid calculations.

$$E_{\mathrm{XC}}^{\mathrm{dRPAgh}} = a_X E_X^{\mathrm{exact}} + (1 - a_X)E_X^{\mathrm{sl}} + E_C^{\mathrm{dRPA}} \quad (8)$$

$$E_{\mathrm{XC}}^{\mathrm{dRPAgdh}} = a_X E_X^{\mathrm{exact}} + (1 - a_X)E_X^{\mathrm{sl}} + a_C E_C^{\mathrm{dRPA}} + (1 - a_C)E_C^{\mathrm{sl}} \quad (9)$$

All energy components are evaluated using self-consistent PBE hybrid orbitals characterized by the fixed a mixing parameter from eq 1.

COMPUTATIONAL DETAILS

The single-point energy calculations were performed using the aug-cc-pVXZ basis sets (denoted here as AXZ), where X was T, Q, 5, or 6. To accelerate the calculations we used the corresponding AXZ-RI-JK and AXZ-RI auxiliary basis sets for the SCF and correlation calculations, respectively. To consider the basis set error we extrapolated the exact exchange and the dRPA correlation parts to the CBS limit according to eqs 10 and 11 similarly to the two-point extrapolations applied in refs 39 and 40

$$E_{\mathrm{CBS}(X,X-1)}^{\mathrm{EX}} = E_{\mathrm{AXZ}}^{\mathrm{EX}} + C_{X,X-1}^{\mathrm{EX}}(E_{\mathrm{AXZ}}^{\mathrm{EX}} - E_{\mathrm{A}(X-1)\mathrm{Z}}^{\mathrm{EX}}) \quad (10)$$

$$E_{\mathrm{CBS}(X,X-1)}^{\mathrm{dRPAc}} = E_{\mathrm{AXZ}}^{\mathrm{dRPAc}} + C_{X,X-1}^{\mathrm{dRPAc}}(E_{\mathrm{AXZ}}^{\mathrm{dRPAc}} - E_{\mathrm{A}(X-1)\mathrm{Z}}^{\mathrm{dRPAc}}) \quad (11)$$

where $C_{4,3}^{\mathrm{EX}} = 0.274$, as well as $C_{4,3}^{\mathrm{dRPAc}}$ is equal to 0.917, 0.856, and 0.867 for (dRPAc)@HF, (dRPAc)@PBE, and (dRPAc)@PBE0.25, respectively.

The dRPA and RPAX2 single-point energies were calculated using the Mrcc program code.[41] For comparison, the dispersion corrected double hybrid energies were partly taken from the literature and partly calculated with the Orca 3.0.1[42] quantum chemistry program using the ATZ basis set with the auxiliary ATZ-RI-JK and ATZ-RI (denoted as ATZ/JK and ATZ/C in Orca) basis sets.

TEST SETS

For quick testing, we suggest a very small but representative test set (sHC5) from five reactions of ethylene, acetylene, propane, propene, and butadiene taken from ref 43. The reactions represent $\pi \rightarrow \sigma$ bond transformations of sp^2 or sp carbon atoms in the molecules, protobranching reactions, and σ- or π-conjugation breaking reactions. The optimized B3LYP/6-31G(2df,p) geometries of these molecules were taken from the NIST Computational Chemistry Comparison and Benchmark Database.[44] For reference energies, we calculated high-quality extrapolated CCSDT(Q)-full/CBS energies. (This test set is used in Figures 1, S1 and Tables 1, S1, S2.)

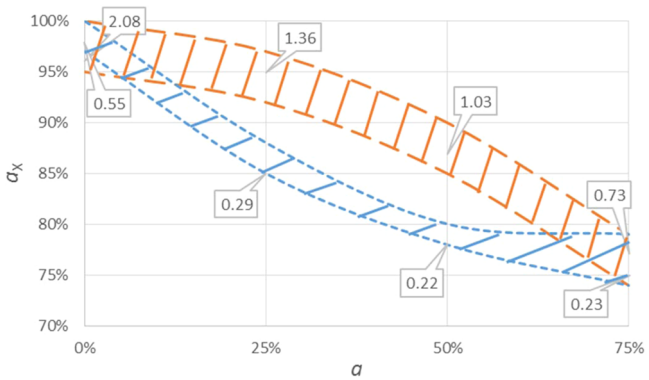

Figure 1. The ranges for the optimal exact exchange mixing parameters a and a_X of dRPA hybrid applied to sHC5 and BH6 test sets. The orange area (with long dashed line borders) stands for the BH6 set (within +0.2 kcal mol^{-1} deviation from the locally minimal MAD values−upper notes), and the blue area (with short dashed line borders) stands for the sHC5 set (within +0.02 kcal mol^{-1} deviation from the locally minimal MAD − lower notes).

For testing the performance of theoretical methods, a convenient hierarchy of reaction classes (RCs) for hydrocarbons was constructed as isogyric (RC1) ⊇ isodesmic (RC2) ⊇ hypohomodesmotic (RC3) ⊇ homodesmotic (RC4) ⊇ hyperhomodesmotic (RC5).[45] The products of each reactions successively conserve larger molecular fragments of the reagents. In isogyric reactions, the total number of electron pairs is conserved. For example the bond separation reactions of hydrocarbons with hydrogen molecules resulting in methane molecules fit into the RC1 reaction class. In isodesmic reactions, the bond orders (single, double, and triple) are also conserved. The bond separation reactions of hydrocarbons with methane molecules yielding diatomic ethane, ethene, and ethyne molecules fit into the RC2 reaction class. In hypohomodesmotic reactions, the reactants and products contain equal numbers of carbon atoms in the same formal hybrid states, and equal numbers of hydrogen atoms are attached. The bond separation reactions of hydrocarbons with diatomic ethane, ethene, and ethyne molecules, resulting in six kind of triatomic hydrocarbons and neopentane as shown in ref 45, fit into the RC3 reaction class. In homodesmotic reactions, the reactants and products contain equal numbers from each possible type of carbon−carbon bonds [C_{sp3}−C_{sp3}, C_{sp3}−C_{sp2}, C_{sp3}−C_{sp}, C_{sp2}−C_{sp2}, C_{sp2}−C_{sp}, C_{sp}−C_{sp}, C_{sp2}=C_{sp2}, C_{sp2}=C_{sp},

DOI: 10.1021/acs.jctc.5b00420
J. Chem. Theory Comput. XXXX, XXX, XXX−XXX

Table 1. Benchmark-Quality Estimated Full CCSDT(Q)/CBS Reaction Energies (kcal mol^{-1}) and Self-Consistent dRPA@HF, dRPA@PBE0.25, dRPA@PBE, dRPAh, and dRPA75 (Eq 12) Deviations from Benchmark Energies ($E - E_{CBS}^{CCSDT(Q)}$) of the sHC5 Set[f]

	system	$E_{CBS}^{CCSDT(Q)}$	$\Delta E_{CBS}^{dRPA@HF}$	$\Delta E_{CBS}^{dRPA@PBE0.25}$	$\Delta E_{CBS}^{dRPA@PBE}$	ΔE_{CBS}^{dRPAh}	ΔE_{CBS}^{dRPA75}
1	$C_2H_4 + 2CH_4 \rightarrow 2C_2H_6$	−21.32	−2.02	−0.16	1.63	1.23	0.76
2	$C_2H_2 + 2CH_4 \rightarrow C_2H_4 + C_2H_6$	−30.82	−2.85	−1.07	0.48	−1.27	−0.05
3	$C_3H_8 + CH_4 \rightarrow 2C_2H_6$	2.08	−0.39	−0.24	−0.18	0.04	−0.14
4	$C_3H_6 + CH_4 \rightarrow C_2H_4 + C_2H_6$	4.81	−0.34	−0.51	−0.80	−0.35	−0.10
5	$C_4H_6 + 2CH_4 \rightarrow 2C_2H_4 + C_2H_6$	13.06	−0.98	−1.27	−1.88	−0.44	−0.07
	MD[a]		−1.32	−0.65	−0.15	−0.17	0.08
	MAD[b]		1.32	0.65	0.99	0.66	0.23
	CSSD[c]		1.09	0.50	1.32	0.91	0.38
	Min[d]		−2.85	−1.27	−1.88	−1.27	−0.14
	Max[e]		−0.34	−0.16	1.63	1.23	0.76

[a]Mean deviation. [b]Mean absolute deviation. [c]Corrected sample standard deviation. [d]Minimum. [e]Maximum. dRPAh denotes the HF + (dRPAc)@PBE hybrid. [f]The CBS extrapolations are based on the ATZ and AQZ energies. The dRPA75 calculations were performed with the ATZ basis set. All calculations were performed on B3LYP/6-31G(2df,p) optimized geometries.

C_{sp}=C_{sp}, C_{sp}≡C_{sp}]. In addition, in hyperhomodesmotic reactions the reactants and products contain equal numbers from each possible type of hydrogen−carbon−carbon−hydrogen bonds [H_3C-CH_2, H_3C-CH, H_2C-CH_2, H_3C-C, H_2C-CH, ...]. The actual test sets for these reaction classes contain 38 reactions, which are divided into three subsets, namely set A: 14 reactions for conjugated hydrocarbons; set B: 22 reactions for nonconjugated hydrocarbons; and set C: two reactions for cyclopentadiene and 1,3-cyclohexadiene. The RC*n* test set requires 64 energy calculations. In this hierarchy, the similarity of the reactants and the products is increasing as we progress from RC1 to RC5, thus the accuracy of the theoretical methods generally increases. Eshuis and Furche[8] reported dRPA@TPSS/cc-pVTZ results for the RC*n* reaction classes. (These test sets are used in Figures 2, S2, S3, S4b-c.)

To illustrate the delocalization errors of semilocal DFT, Johnson et al.[46] suggested a test set of 14 Diels−Alder reactions, abbreviated as DARC. These are condensation reactions of dienes like butadiene, cyclopentadiene, cyclohexadiene, and furane with dienophiles like ethene, ethyne, maleine, and maleimide. The majority of the DFT functionals underestimates the noncovalent intramolecular interactions, which occur in the larger bicyclic and tricyclic products leading to endothermic reaction energy error. Johnson et al. observed a systematic improvement in the calculated reaction energies for functionals which treat fractionally charged systems more correctly (rCAM-B3LYP and MCY3). Based on this observation, it was supposed that the DARC test set is suitable for testing the electron delocalization error in DFT. Our recent study[47] has shown that the DARC test set is not particularly suitable for identifying the delocalization error caused by the self-interaction error, but it is an excellent test set for intramolecular interactions and bond reorganizations. This is because the reactions in the DARC test set are influenced by many effects, e.g., double (ethene) and triple (ethyne) bonds are transformed into single and double bonds, the electron delocalization in the dienes is destroyed, double and triple ring formations, etc.[47] (This test set is used in Figures 3, S5, S6.)

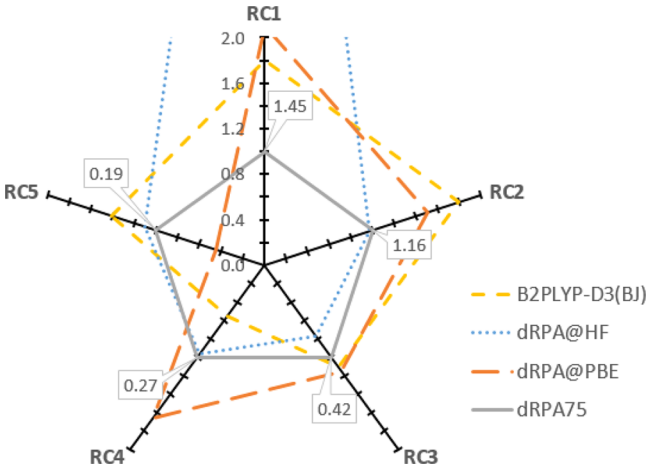

Figure 2. MAD(method)/MAD(dRPA75) ratios of B2PLYP-D3(BJ), dRPA@HF, and dRPA@PBE methods and the dRPA75 MAD values in kcal mol^{-1} for RC1-RC5 *n*-homodesmotic hierarchy of reactions. Smaller ratio means better performance. For the RC1 the dRPA@HF yields a very large, out of chart MAD (11.6 kcal mol^{-1}). Abbreviations: RC1, isogyric; RC2, isodesmic; RC3, hypohomodesmotic; RC4, homodesmotic; RC5, hyperhomodesmotic.

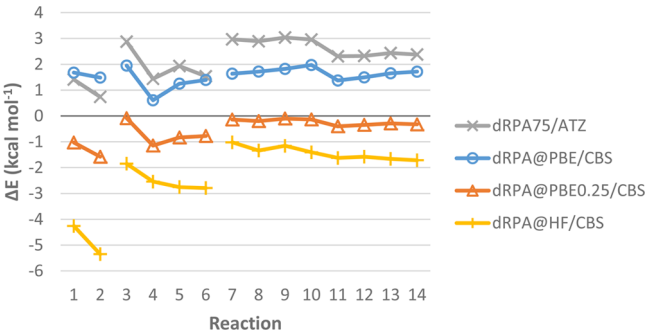

Figure 3. The dRPA75, dRPA@PBE, dRPA@PBE0.25, and dRPA@HF deviations from the benchmark reaction energies of the DARC Diels−Alder reaction test set. Abbreviations: ATZ, aug-cc-pVTZ basis set; CBS, complete basis set.

Lynch and Truhlar proposed a small database consisting of six atomization energies (AE6),[48] which is a representative part of the 109 atomization energies of Database/3.[49] We used this small database with very accurate estimated CCSDT(Q)-full/CBS reference values.[50] We also include the atomization reaction energies of 38 hydrocarbons (the RC0 test set)[45] used for the homodesmotic hierarchy of reactions. Atomization is

DOI: 10.1021/acs.jctc.5b00420
J. Chem. Theory Comput. XXXX, XXX, XXX−XXX

Table 2. Benchmark Quality Estimated Full CCSDT(Q)/CBS Atomization Energies (kcal mol^{-1}) Taken from Ref 50 and dRPA@HF, dRPA@PBE0.25, dRPA@PBE, dRPAh, and dRPA75 Deviations from Benchmark Energies ($E - E_{CBS}^{CCSDT(Q)}$) of the AE6 Set[f]

molecule	$E_{CBS}^{CCSDT(Q)}$	$\Delta E_{CBS}^{dRPA@HF}$	$\Delta E_{CBS}^{dRPA@PBE0.25}$	$\Delta E_{CBS}^{dRPA@PBE}$	ΔE_{CBS}^{dRPAh}	ΔE_{CBS}^{dRPA75}
$C_2H_2O_2$	636.3	−49.0	−29.1	−36.8	−22.4	−17.8
C_3H_4	706.1	−41.8	−29.2	−38.1	−32.5	−25.8
C_4H_8	1153.7	−61.3	−42.5	−54.3	−46.7	−46.5
S_2	104.7	−15.3	−7.5	−8.7	−3.1	−5.9
SiH_4	324.9	−15.0	−8.7	−9.4	−4.1	−16.0
SiO	193.9	−22.9	−13.0	−14.2	−6.5	−8.6
MD[a]		−34.2	−21.7	−26.9	−19.2	−20.1
MAD[b]		34.2	21.7	26.9	19.2	20.1
CSSD[c]		19.3	14.1	18.8	17.9	14.7
Min[d]		−61.3	−42.5	−54.3	−46.7	−46.5
Max[e]		−15.0	−7.5	−8.7	−3.1	−5.9

[a]Mean deviation. [b]Mean absolute deviation. [c]Corrected sample standard deviation. [d]Minimum deviation. [e]Maximum deviation. [f]The CBS extrapolations are based on the ATZ and AQZ energies. Similarly to the EX + dRPAc methods, we extrapolate the PBE0.75 exchange with $\Delta E_{4,3}^{dRPA75x}$ = 0.312 and the (dRPAc)@PBE0.75 with $\Delta E_{4,3}^{dRPAc}$ = 0.837. All calculations were performed on B3LYP/6-31G(2df,p) optimized geometries.

the lowest possible reagent-product similarity class of bond separation energies. (These test sets are used in Tables 2, S4, S5 and Figures 4, S4a.)

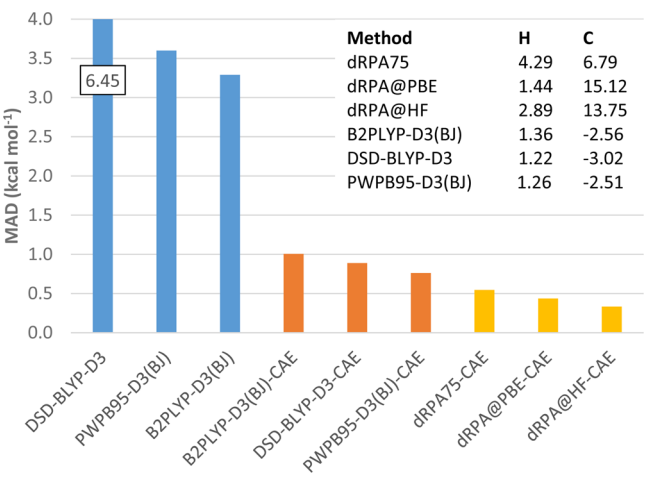

Figure 4. Corrected atomic energies (kcal mol^{-1}) optimized for the atomization energies of the RC0 test set (top-right corner) and mean absolute deviations (MAD) from the benchmark atomization energies of the RC0 set for DSD-BLYP-D3, PWPB95-D3(BJ), and B2PLYP-D3(BJ) without or with corrected atomic energies, as well as dRPA75, dRPA@PBE, and dRPA@HF with corrected atomic energies (calculated with the ATZ basis set).

For testing the performance on reaction barriers, we use the accurately known DBH24 test set,[51] which is composed of four subsets: BH6 for hydrogen transfer; HAT6 for heavy atom transfer; NS6 for nucleophilic substitution; UR6 for unimolecular and recombination reactions. For BH6, we use the estimated CCSDT(Q)-full/CBS reference energy values,[50] and for the other three test sets, we use the energies obtained from the W3.2 and W4 *ab initio* computational thermochemistry protocols, which have a 95% confidence interval well below 0.2 kcal mol^{-1}. We also use the less accurately known but considerably larger HT- and NHT-BH38 reaction barrier test sets.[21] (These test sets are used in Tables 3, 4, S6, S7 and Figures 5, S8.)

For testing the performance on intermolecular interactions, we used the noncovalent complexes of the NCCE31 test set[5253] (with MC-QCISD/3 reference energy values), which contains six hydrogen-bonded, seven charge transfer, six dipole−dipole, seven weak interacting, and five $\pi-\pi$ stacking complexes. We also included the biologically important complexes of the S22 database[5455] (with estimated CCSD(T)/CBS reference values), which contains seven hydrogen bonded complexes, eight dispersion dominated complexes, and seven mixed complexes. (These test sets are used in Figures 6, 7, S9 and Table S8.)

Furthermore, we used four databases to test the performance for intramolecular interactions. The aliphatic dispersion interaction is tested using a set of alkane conformers (ACONF)[56] which compares the relative energies among two butane, three pentane, and 11 hexane conformers with W1h-val reference values. A set of cysteine conformers (CYCONF),[57] a set of phenylalanine-glycine-glycine tripeptide conformers (PCONF),[58] and a set of sugar derivatives (SCONF)[59] test various kinds of intramolecular hydrogen bonds, all with estimated CCSD(T)/CBS reference values. (These test sets are used in Figure 8 and Table S9.)

Common semilocal density functional approximations underestimate the energy of systems with fractional charge.[60] Thus, the delocalization of electrons is preferred, and this error is called delocalization error. Fractional charge is present e.g. in transition states and leads to the underestimation of the barrier heights. The prototype indicator of the delocalization error is the potential energy curve of the dissociating H_2^+ molecule ion.[61] Similarly, the energy of systems with fractional spin is overestimated by the static correlation error. Fractional spin can occur, e.g. by the breaking of chemical bonds. The prototype indicator of this error is the potential energy curve of the dissociating H_2 molecule.[61] (These systems are used in Figure S7 and Table S3.)

RESULTS AND DISCUSSION

New Dual-Hybrid Method. Obtaining good results for chemical reaction energies and barriers with the same functional is a challenge for semilocal DFT methods. We have selected two very small but representative test sets (sHC5 and BH6) to develop a new method for both reaction energies and barriers. As we develop a model chemistry which is useful for the largest molecules possible, we use the relatively small ATZ basis set, which gives consistent results. We present all the details of the parameter optimization in Tables S1a-d, S6a-d

DOI: 10.1021/acs.jctc.5b00420
J. Chem. Theory Comput. XXXX, XXX, XXX−XXX

Table 3. Benchmark Quality Estimated Full CCSDT(Q)/CBS Reaction Barrier Heights (kcal mol^{-1}) Taken from Ref 50 and dRPA@HF, dRPA@PBE0.25, dRPA@PBE, dRPAh, and dRPA75 Deviations from Benchmark Energies ($E - E_{CBS}^{CCSDT(Q)}$) of the BH6-DBH24 Set[f]

	system	$E_{CBS}^{CCSDT(Q)}$	$\Delta E_{CBS}^{dRPA@HF}$	$\Delta E_{CBS}^{dRPA@PBE0.25}$	$\Delta E_{CBS}^{dRPA@PBE}$	ΔE_{CBS}^{dRPAh}	ΔE_{CBS}^{dRPA75}
1	$OH + CH_4 \rightarrow [HOHCH_3]$	6.02	7.57	1.20	0.91	−7.97	−0.13
2	$H_2O + CH_3 \rightarrow [HOHCH_3]$	19.46	5.40	−0.70	−2.58	−11.97	−1.72
3	$H + OH \rightarrow [HOH]$	10.78	5.02	−0.29	−1.99	−8.28	−0.19
4	$H_2 + O \rightarrow [HOH]$	12.88	6.90	1.16	0.70	−6.79	−0.57
5	$H + H_2S \rightarrow [HHSH]$	3.78	3.40	0.99	0.06	−3.37	0.82
6	$H_2 + HS \rightarrow [HHSH]$	16.97	3.64	2.68	3.70	−0.20	1.33
	MD[a]		5.32	0.84	0.13	−6.43	−0.07
	MAD[b]		5.32	1.17	1.66	6.43	0.79
	CSSD[c]		1.68	1.21	2.26	4.12	1.07
	Min[d]		3.40	−0.70	−2.58	−11.97	−1.72
	Max[e]		7.57	2.68	3.70	−0.20	1.33

[a]Mean deviation. [b]Mean absolute deviation. [c]Corrected sample standard deviation. [d]Minimum. [e]Maximum. [f]The CBS extrapolations are based on the ATZ and AQZ energies. The dRPA75 calculations were performed with the ATZ basis set. All calculations were performed on B3LYP/6-31G(2df,p) optimized geometries.

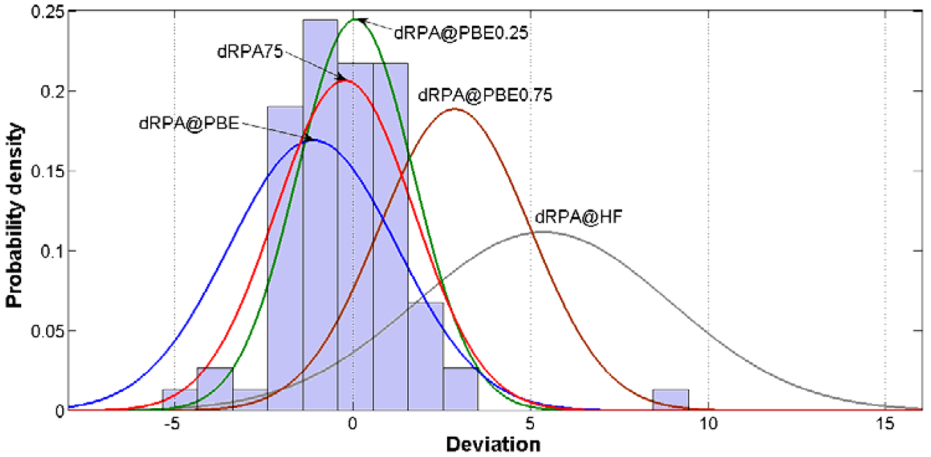

Figure 5. Fitted normal distributions for the dRPA@PBE, dRPA75, dRPA@PBE0.25, dRPA@PBE0.75, and dRPA@HF deviations (kcal mol^{-1}) from the benchmark reaction barrier heights of the BH76 set and histogram for dRPA75.

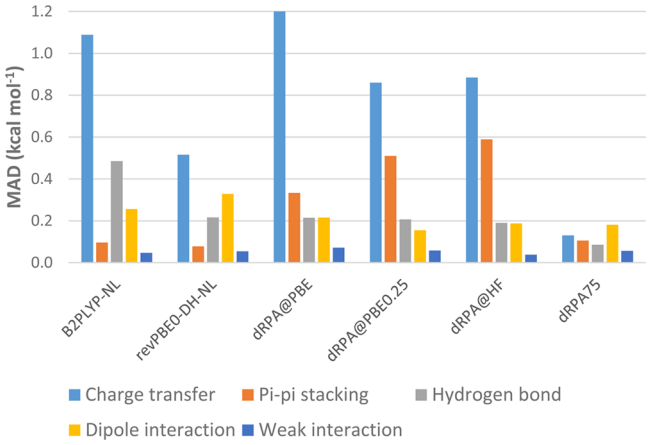

Figure 6. The mean absolute deviations (MAD) from the benchmark interaction energies of the complexes of NCCE31 set for nonlocal VV10 corrected B2PLYP and revPBE0-DH (taken from ref 69), as well as dRPA@PBE, dRPA@PBE0.25, dRPA@HF, and dRPA75 (calculated with the ATZ basis set).

and Figure S1 of the Supporting Information. For either the sHC5 or the BH6 test set, the global optimum in the a, a_X, and a_C parameter space of eqs 1 and 9 leads to only one accurate and precise dual-hybrid method (shortened as dRPA75).

$$E_{XC}^{dRPA75} = (0.75E_X^{exact} + 0.25E_X^{PBE} + E_C^{dRPA})@PBE0.75/ATZ \quad (12)$$

For this hybrid, we use a PBE0.75 global hybrid orbital reference with $a = 0.75$ in eq 1. The beneficial effects of such a large 0.7−0.8 fraction of exact exchange were also described in refs 25 and 30. The same 0.75 fraction is optimal for a_X in eq 8 combined with full dRPA correlation ($a_C = 1$ in eq 9).

Notice that mixing semilocal PBE correlation with the fully nonlocal dRPA correlation does not lead to improvement thus $a_C = 1$ is optimal in eq 9. Figure 1 shows the distribution of the optimal values (within 0.2 kcal mol^{-1} deviation from the locally minimal MAD) for the sHC5 and BH6 test sets in the a, a_X space for $a_C = 1$. The overlapping regions in Figure 1 are around the dRPA@PBE and dRPA75 methods, but the latter has improved accuracy for both the reaction energies and the barriers heights. This finding underlines the good properties of PBE hybrid orbitals with a large fraction of exact exchange discussed in the literature.[25,30]

Also notice that the optimal $(1 - a_X) = 0.25$ weight factor of the nondynamic correlation correction ($E_X^{sl} - E_X^{exact}$) to the exchange-correlation energy is much smaller for dRPA75 than

DOI: 10.1021/acs.jctc.5b00420
J. Chem. Theory Comput. XXXX, XXX, XXX−XXX

for the popular global hybrids (cf. 0.80 for B3LYP, 0.75 for PBE0.25, 0.46 for M06-2X) or double hybrids (0.5 for PWPB95, 0.47 for B2PLYP, 0.45 for mPW2PLYP). Table S1a and Figure S1 show a local optimum about 53% dRPA + 47% PBE correlation, which agrees well with our earlier suggestion of dRPAgdh@PBE (a = 0, a_X = 0.5, a_C = 0.5 in eq 9),[14] but this functional shows considerably poorer performance for the sHC5 test set than the new dRPA75 hybrid. In the following, we present the performance of this new approach on the test sets introduced above.

Reaction Energies. Table 1 shows the estimated CCSDT-(Q)-full/CBS reference energies and dRPA energy deviations for the sHC5 test set. The results show a particularly good performance for dRPA75/ATZ. For the sHC5 reaction energies, dRPA shows quite rapid basis set convergence as shown in Tables S2a and S2b. We note also that the RPAX2@PBEx/ATZ, AQZ, and A5Z energies are very accurate and precise (cf. Table S2c).

Figure 2 shows the radar or polar chart for the relative performance represented by the MAD(method)/MAD(dRPA75) ratios of B2PLYP-D3(BJ), dRPA@HF, dRPA@PBE methods and the dRPA75 MAD values in kcal mol^{-1} for RC1-RC5 n-homodesmotic hierarchy of reactions. The double hybrid functionals perform similarly to each other, so we show only the typical performance of the B2PLYP-D3(BJ) method. For the RC1 reaction class, dRPA75 is the best among the methods shown in Figure 2, while the MAD(dRPA@HF)/MAD(dRPA75) = 8 is out of the chart. (The error distributions are shown in Figure S2.) The dRPA@TPSS/cc-pVTZ results (MAD = 6.7 kcal mol^{-1})[8] are also considerably poorer than our dRPA75 results. The commonly used DFT methods like M06-2X and B3LYP yield large MADs (9.1 and 11.9 kcal mol^{-1}, respectively). For the RC2 reaction class, dRPA75 is the best again and dRPA@HF has similar performance, while the dRPA@PBE and B2PLYP-D3(BJ) yield larger deviations. dRPA@TPSS/cc-pVTZ,[8] M06-2X, and B3LYP yield MAD = 2.1, 2.4, and 4.2 kcal mol^{-1}, respectively. For the RC3 reaction class, the performance of dRPA75 improves further, and the other methods discussed here have similar MADs within 20%. For RC1-RC5, the MAD of dRPA75 decreases monotonically. Practically, all the methods shown in Figure 2 perform well for RC3-RC5. The B3LYP and M06-2X methods yield accurate results with a surprisingly low precision. For example the highly empirical M06-2X functional might yield errors above 2 kcal mol^{-1} for the RC4-5 reaction classes.

We show detailed results for the A, B, and C subsets of the five reaction classes in Figures S3a-f for dRPA@HF, dRPA@PBE, dRPA75, and dRPA@TPSS/cc-pVTZ[8] and the D3 dispersion corrected B2PLYP, PWPB95, and DSD-BLYP (taken from ref 8). For the isogyric RC1A test set, the D3 dispersion corrected double hybrid methods perform about the same as dRPA75, but dRPA75 shows much better performance for the RC1B and RC1C test sets. For the RC4 and RC5 reaction classes, the MADs of dRPA75 are in the insignificant range, 0.1−0.3 kcal mol^{-1}.

Comparison of Figures S4b and S4c shows that the basis set convergence of the RC1 reaction energies is considerably slower than that of the RC2 reaction energies. For detailed analysis of the basis set convergence of the dRPA correlation energies, see ref 40.

Next we test the performance of the dRPA method with various reference orbitals on the DARC reaction energy test set. Figure 3 shows that our new dRPA75 method has about 2 kcal mol^{-1} endothermic reaction energy error with a good precision (CSSD = 0.7 kcal mol^{-1}). dRPA@PBE0.75 shows an overbinding error very similar (the average difference is around 0.1 kcal mol^{-1}) to dRPA@HF (cf. Figure S5a). Consequently, the 25% of PBE exchange in PBE0.75 leads to the above-mentioned underbinding error. The more diffuse PBE electron densities result in more endothermic reaction energies than the compact HF electron densities (cf. Figures S5a and S5b). The AQZ or ATZ basis set errors shift the DARC reaction energies in the exothermic direction (cf. Figures S5a-c). The less compact PBE electron density yields larger dRPA basis set error than the more compact HF electron density.

Our recent results show that the systematic endothermic error of the dRPA@PBE/CBS reaction energies can be efficiently compensated by the systematic exothermic error of the AQZ basis set (MD = 0.08 kcal mol^{-1}, MAD = 0.32 kcal mol^{-1} and CSSD = 0.42 kcal mol^{-1}; see also Figure S5b) because on more diffuse reference orbitals the self-correlation error of the dRPA correlation overstabilizes more the chemical delocalization in the reactants (see ref 47), and the cusp error stabilizes more the diffuse electron densities in the products (see ref 40). Mixing PBE exchange with 0.25 fraction of exact exchange can also compensate the systematic endothermic error of dRPA@PBE/CBS reaction energies (cf. MD = −0.53 and MAD = 0.53 kcal mol^{-1} in ref 47). The more expensive RPAX2@PBEx/ATZ calculations lead to very precise reaction energies with a small exothermic error (MD = −0.83, MAD = 0.83, in ref 47). Standard functionals like B3LYP, PBE, PBE0, TPSS, or TPSSh yield inaccurate and imprecise results for the DARC reaction energies characterized by MAD = 15 kcal mol^{-1} and CSSD = 5 kcal mol^{-1}.[62] The highly empirical M06-2X functional is relatively accurate (MD = 1.92 kcal mol^{-1})[62] but considerably less precise (CSSD = 2 kcal mol^{-1}) than the new dRPA75. The best performing double hybrid functionals show similar performance to dRPA methods presented here as shown in Figure S6, but they are far from the accuracy and precision of the dRPA@PBE/AQZ for the DARC test set.

Delocalization and Static Correlation Errors. The delocalization error of the semilocal density functionals can be well represented by the dissociation of homonuclear diatomic radical cations (i.e., H_2^+) as the semilocal DFT incorrectly stabilizes the fractionally charged product over the integer charged products.[29] In Figure S7a and Table S3a, we show the dRPA@HF, dRPA@PBE0.25, dRPA@PBE, and dRPA75 errors. Our earlier results show that the one-electron self-interaction error free RPAX2@PBEx yields perfect binding curve for H_2^+.[47]

Another serious error of semilocal DFT is the so-called static correlation error represented by the H_2 binding energy curve. Figure S7b and Table S3b show the dRPA@HF, dRPA@PBE0.25, dRPA@PBE, and dRPA75 errors. All dRPA methods discussed here underbind the H_2 molecule. The underbinding increases from 2 kcal mol^{-1} up to 8 kcal mol^{-1} in the order of dRPA@PBE < dRPA75 < dRPA@HF (Table S3b). Again the RPAX2@PBEx gives the best agreement with the reference curve.[47]

Atomization Energies. The underbinding error of dRPA/CBS is very large, around 20 kcal mol^{-1} as shown in Table 2 and Table S4a-b for the AE6 test set. The underbinding error of the ATZ basis set increases this error further by 11 kcal mol^{-1} on average. It was shown in the literature that range separation can diminish the atomization energy errors.[63] Another possibility is the AXK correction, but still it has similar

DOI: 10.1021/acs.jctc.5b00420
J. Chem. Theory Comput. XXXX, XXX, XXX−XXX

atomization energy errors to TPSS.[34] We have also calculated the RPAX2@PBEx/ATZ, AQZ, and A5Z atomization energies (Table S4c) and found that the CBS extrapolated atomization energies are quite accurate and precise for the AE6 test set. The RPAX2@PBEx atomization energies also converge well with the basis set quality. The underbinding error of the A5Z basis set efficiently compensates the small overbinding error of the RPAX2@PBEx method.

Next we analyze the errors of the calculated atomization energies for the 38 hydrocarbons in the RC0 test set. Table S5 shows the statistical data of the deviations and the relative deviations of the calculated atomic energies from the reference energies for dRPA@HF, dRPA@PBE, dRPA75, and B2PLYP-D3(BJ). The dRPA75 method is particularly precise for atomization energies (CSSD = 0.07%) but underbinds the molecules by slightly more than 5%. The B2PLYP-D3(BJ) method is very accurate but much less precise than the dRPA75. The dRPA@PBE and dRPA@HF methods are considerably less precise. This means that dRPA75 atomization energy error is systematic, even more systematic than that of the accurate B2PLYP-D3(BJ), thus the relative energies of the molecules are quite correct leading to good chemical reaction energies as it was the case for the RC*n* test sets analyzed above.

As we stated previously: "The atomization energy errors of a density functional can strongly magnify minor errors in its spin-polarization dependence which are of little importance for other properties of many molecules and solids. Thus, density functionals should not be judged primarily by their atomization energy errors, but by a wider spectrum of tests.".[64]

Due to the systematic nature of the atomization energy errors an efficient correction is possible by optimized atomic energies (CAE = corrected atomic energies).[65] Figure 4 shows these corrected atomization energies for dRPA@HF, dRPA@PBE, dRPA75, and D3 dispersion corrected B2PLYP methods. (Notice the much smaller corrections for double hybrids compared to dRPA.) These *a posteriori* fitted atomic energies considerably reduce the atomization energy errors for the RC0 test set, but the imprecision of the double hybrid methods cannot be corrected as efficiently as the more systematic errors of the dRPA methods. Excellent results can be obtained from dRPA75-CAE, dRPA@PBE-CAE, and dRPA@HF-CAE.

As we noted for the AE6 test set, the dRPA atomization energies are very sensitive to the basis set error. In Figure S4a, we show the very large basis set errors of (dRPAc)@HF with the ATZ basis sets for nine instances and the convergence of the atomization energies as a function of the increasing cardinal numbers up to six. Even the A6Z basis set shows considerable dRPAc@HF atomization energy error for larger hydrocarbons like pentane or other pentane derivatives.

Barrier Heights. Popular DFT methods seriously underestimate the reaction barrier heights, while the HF method seriously overestimates them. Some kind of uncertain error compensation might lead to somewhat improved results for global hybrid functionals, but the improvement is unreliable. Also the large fraction of exact exchange needed for good reaction barriers[66] worsens the results for reaction energies. Application of a very large number of empirical parameters might lead to somewhat improved results at the cost of a wavy energy surface (e.g., M05-2X and M06-2X functionals).

Table 3 shows the estimated CCSDT(Q)-full/CBS reference energies and deviations for various dRPA methods for the BH6-DBH24 test set. These results show the typical dRPA@HF errors (in agreement with the values reported earlier[20,66]). The hybrid dRPAh fails to deliver good results for reaction barriers. This is because the average HF/CBS exchange energy error is 12.5 kcal mol^{-1} in agreement with ref 66. This error is decreased by the (dRPAc)@HF correlation energy for the reaction barriers by about 7 kcal mol^{-1}. Replacing the HF orbitals by PBE orbitals increases the average exact exchange energy error to 19.1 kcal mol^{-1}. This error is almost perfectly compensated by the average (dRPAc)@PBE correlation energy for the reaction barriers leading to very accurate dRPA@PBE energies. However, correcting the too small average HF/CBS exchange energy error with the same average (dRPAc)@PBE correlation energy for the reaction barriers leads to serious underestimation of the barrier heights, and this makes the dRPAh method unsuitable for reaction barrier height calculations. Comparison of the barrier heights in Tables 3, S7a and S7b shows that the calculated dRPA barrier heights are quite insensitive to the basis set errors, and the ATZ results show a few tenths of kcal mol^{-1} errors, thus these ATZ and AQZ results are practically converged with respect to the basis set size. Inspection of Table 3 reveals that despite the excellent accuracy, the dRPA@PBE/CBS results are quite imprecise. The dRPA@PBE0.25/CBS results are less accurate but more precise than the dRPA@PBE/CBS results.

The most accurate and precise barrier heights by far are obtained again with dRPA75/ATZ. These results are very close to the CBS results, as good as the CBS-Q, MC-QCISD/3 results, much better than the MP2, MP3, MP4, CCD, or QCISD(T) results[48] and also considerably better than the results obtained with the MPWB1K method empirically optimized for reaction barriers (MAD = 1.32 kcal mol^{-1}).[67] We have also calculated the considerably more expensive RPAX2@PBEx/ATZ, AQZ, and A5Z barrier heights (see Table S7c) and obtained a systematic overestimation independently of the basis set quality. This shows one of the limitations of the RPAX2@PBEx method.

The overall good performance of the dRPA75/ATZ method for reaction barriers can be followed in Tables S7d-f for the HAT6-, NS6-, and UR6-DBH24 test sets. The overall performances for the 24 barrier heights are summarized in Table 4. The best method is dRA75/ATZ followed closely by dRPA@PBE0.25/ATZ. The best range-separated RPA shows larger MAD (2.83 kcal mol^{-1}) for the DBH24 test set.[63]

We have also included larger but less accurately known (for comparison see Table S7g) reaction barrier test sets into our study: the NHT-BH38 (Table S7h) and HT-BH38 (Table S7i) test sets of 76 barrier heights. The error distributions of the dRPA methods for the BH76 test set is shown in Figure 5. The

Table 4. Statistics of the DBH24 Database for dRPA@HF, dRPA@PBE0.25, dRPA@PBE, and dRPA75[f]

	$\Delta E_{ATZ}^{dRPA@HF}$	$\Delta E_{ATZ}^{dRPA@PBE0.25}$	$\Delta E_{ATZ}^{dRPA@PBE}$	ΔE_{ATZ}^{dRPA75}
MD[a]	5.87	0.25	−0.95	−0.08
MAD[b]	5.87	1.66	2.11	1.42
CSSD[c]	4.46	1.90	2.37	1.72
Min[d]	1.00	−2.72	−5.17	−2.24
Max[e]	18.87	3.90	3.95	3.14

[a]Mean deviation. [b]Mean absolute deviation. [c]Corrected sample standard deviation. [d]Minimum. [e]Maximum. [f]With estimated CCSDT-(Q)-full/CBS reference values for the BH6 subset, W3.2 and W4 reference values otherwise. All calculations were performed with the ATZ basis set.

DOI: 10.1021/acs.jctc.5b00420
J. Chem. Theory Comput. XXXX, XXX, XXX−XXX

new dual-hybrid dRPA75 is among the best performing methods (MAD = 1.38 kcal mol^{-1}), and it is also better than the AXK results (MAD = 1.63 kcal mol^{-1}).[34] Note that although dRPA@PBE0.25 looks slightly better (MAD = 1.37 kcal mol^{-1}) than dRPA75 in Figure 5, the reference values have 0.3−0.4 kcal mol^{-1} error, which makes this comparison uncertain (cf. the DBH24 and BH76 results in Figure S8a). (For the sake of completeness, the deviations from the benchmark reaction energies of the BH76 test set are compared in Figure S8b.)

Inter- and Intramolecular Interactions. First we tested our new method (dRPA75) on various types (charge transfer, $\pi-\pi$ stacking, hydrogen bond, dipole interaction, and weak interaction) of intermolecular interactions of the NCCE31 database. Figure 6 shows the double hybrid GGA with nonlocal correction (taken from ref 67); dRPA@HF, dRPA@PBE, dRPA@PBE0.25, and dual-hybrid dRPA75 mean absolute deviations from the benchmark noncovalent complexation energies of the NCCE31 database. dRPA75 is much more accurate and precise for charge transfer interaction energies than any other method shown in Figure 6. The situation is similar for $\pi-\pi$ stacking and hydrogen bond energies. The dispersion corrected double hybrid B2PLYP-NL or revPBE0-DH-NL functionals show considerably poorer performance than dRPA75. For dipole and weak interactions, dRPA75 is quite competitive with the other methods in Figure 6. The dual-hybrid dRPA75 gives well-balanced, accurate, and precise interaction energies for all types of complexes in this test set (all MAD values are below 0.2 kcal mol^{-1}). The detailed results for the components of the NCCE31 test set can be found in Tables S8a-f.

Then we also examined the performance of our new method on the S22 test set that contains several biologically important weak interactions. Figure 7 shows the MADs of the D3

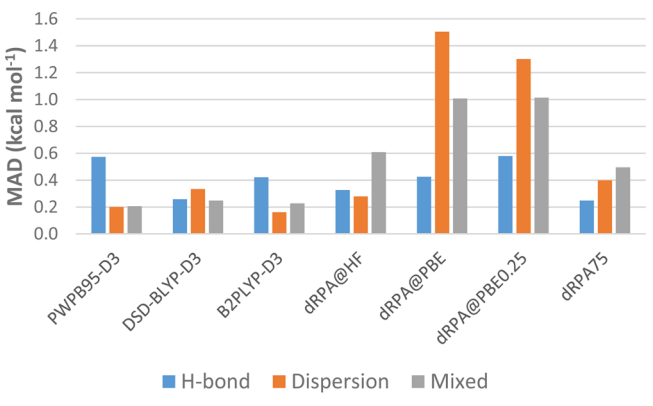

Figure 7. The mean absolute deviations (MAD) from the benchmark interaction energies of the complexes of S22 set for D3 dispersion corrected PWPB95, DSD-BLYP, and B2PLYP (taken from the GMTKN30 database), as well as dRPA@HF, dRPA@PBE, dRPA@PBE0.25, and dRPA75 (calculated with the ATZ basis set).

dispersion corrected double hybrid GGA, dRPA, and dual-hybrid dRPA75 from the benchmark interaction energies of the S22 database. Figure S9 shows that the dRPA@PBE/ATZ and dRPA@PBE0.25/ATZ overestimate the dissociation energies of the dispersion bonded and mixed complexes (Figure S9). The origin of this overbinding is the basis set error. In this respect, our results are in a perfect agreement with the dRPA@PBE/ATZ results of Eshuis and Furche.[68] The mean overbinding basis set error of the dRPA@PBE/ATZ energies is around 1.7 kcal mol^{-1} in ref 68. The dRPA@HF and the dual-hybrid dRPA75 methods with the ATZ basis set give reasonable results for the S22 complexes. The basis set error for the more compact HF and PBE0.75 reference determinants is smaller than the basis set error for the PBE reference determinant as it was recently observed in ref 40. The estimated underbinding MD of the dRPA75/CBS is around 1 kcal mol^{-1}, and this is larger than the MDs of the dRPA@PBE or dRPA@PBE0.25 methods.[19] However, notice that the systematic error cancellation in the dRPA75 works well for the S22 test set too.

The calculation of the intramolecular interactions is even more challenging than that of the intermolecular interactions because of the nonbonded electron density overlaps as we have pointed out previously for the Diels−Alder reaction energies. To test the performance of the methods for intramolecular interactions, we have selected the well tested ACONF, CYCONF, PCONF, and SCONF test sets from the GMTKN30 database. For comparison, we have selected three well-performing double hybrid functionals, the D3 dispersion corrected B2PLYP, PWPB95, and DSD-BLYP. The performance of these functionals is known in the GMTKN30 database. Figure 8 shows that the performances of dRPA@HF, dRPA@

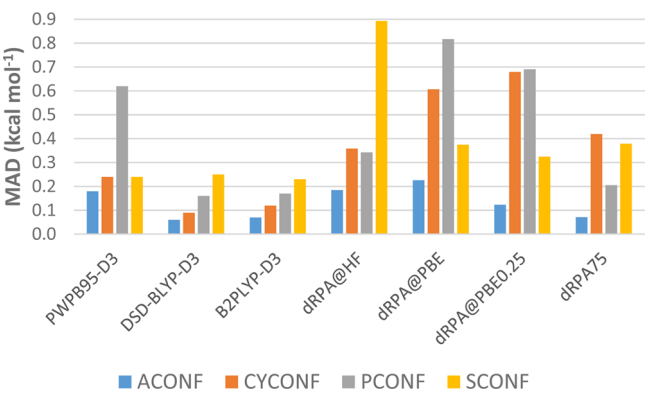

Figure 8. The mean absolute deviations (MAD) from the benchmark relative conformational energies of the ACONF, CYCONF, PCONF, and SCONF test sets for D3 dispersion corrected PWPB95, DSD-BLYP, and B2PLYP (taken from the GMTKN30 database), as well as dRPA@HF, dRPA@PBE, dRPA@PBE0.25, and dRPA75 (calculated with the ATZ basis set).

PBE, and dRPA@PBE0.25 are not particularly good for these energies. However, dRPA75 dual-hybrid gives excellent results for ACONF and PCONF test sets and performs reasonably well for the other two test sets. Several double hybrids like B2PLYP-D3 and DSD-BLYP-D3 perform better for the CYCONF and SCONF test sets. Notice that the 0.2 kcal mol^{-1} deviation is so small that it can be smaller than the errors in the reference energies. Further details about the performance of the new dual-hybrid dRPA75 can be found in Tables S9a-d.

In Table 5, we summarize the MAD values (in kcal mol^{-1}) for 27 test sets. We selected the B2PLYP-D3(BJ), dRPA@HF, dRPA@PBE, dRPA@PBE0.25, and dRPA75 methods for comparison. The B2PLYP-D3(BJ) results are taken from the literature. Inspection of the results shows that the dRPA75 method shows excellent overall performance (the smallest MAD values are in bold), and it is applicable for a wide range of chemical problems.

DOI: 10.1021/acs.jctc.5b00420
J. Chem. Theory Comput. XXXX, XXX, XXX−XXX

Table 5. Summary of Mean Absolute Deviations (MAD in kcal mol^{-1}) from Reference Energies for Dispersion Corrected B2PLYP-D3(BJ), dRPA@HF, dRPA@PBE0.25, dRPA@PBE, and dRPA75[g]

	B2PLYP-D3	dRPA@HF	dRPA@PBE0	dRPA@PBE	dRPA75
Reaction Energies					
sHC5		1.32[a]	0.65[a]	0.99[a]	**0.23**[b]
RC1	2.62[c]	11.60[b]		3.05[b]	**1.45**[b]
RC2	2.09[c]	**1.13**[b]		1.75[b]	**1.16**[b]
RC3	**0.46**[c]	**0.32**[b]		**0.48**[b]	**0.42**[b]
RC4	**0.15**[c]	**0.26**[b]		0.45[b]	**0.27**[b]
RC5	**0.27**[c]	**0.21**[b]		**0.09**[b]	**0.19**[b]
DARC	5.03[d]	2.22[a]	**0.53**[a]	1.55[a]	2.23[b]
Atomization Energies					
AE6	1.90[c]	34.20[a]	21.70[a]	26.90[a]	30.70[b]
RC0	3.29[c]	102.30[b]		97.51[b]	75.04[b]
	(0.96)[e]	(**0.35**)[e]		(**0.40**)[e]	(**0.55**)[e]
Barrier Heights					
BH6	2.28[d]	5.04[b]	1.73[b]	2.24[b]	**0.79**[b]
HAT6	2.86[d]	11.57[b]	**2.17**[b]	2.29[b]	**2.00**[b]
NS6	3.63[d]	2.72[b]	**1.56**[b]	2.93[b]	**1.75**[b]
UR6	**0.73**[d]	4.17[b]	**1.17**[b]	**0.97**[b]	**1.16**[b]
DBH24 total	2.38[d]	5.87[b]	1.66[b]	2.11[b]	**1.42**[b]
NT-BH38	2.83[d]	5.49[b]	**1.30**[b]	2.28[b]	1.97[b]
HT-BH38	2.20[d]	5.20[b]	1.45[b]	1.96[b]	**0.80**[b]
BH76 total	2.51[d]	5.35[b]	**1.37**[b]	2.12[b]	**1.38**[b]
Intermolecular Interactions					
HB6	0.49[f]	0.19[b]	0.21[b]	0.22[b]	**0.09**[b]
CT7	1.09[f]	0.88[b]	0.86[b]	2.37[b]	**0.13**[b]
DI6	**0.26**[f]	**0.19**[b]	**0.16**[b]	**0.22**[b]	**0.18**[b]
WI7	**0.05**[f]	**0.04**[b]	**0.06**[b]	**0.07**[b]	**0.06**[b]
PPS5	**0.10**[f]	0.59[b]	0.51[b]	0.33[b]	**0.11**[b]
NCCE31 total	0.42[f]	0.38[b]	0.36[b]	0.69[b]	**0.11**[b]
H-bond (S22)	0.42[d]	**0.33**[b]	0.58[b]	0.43[b]	**0.25**[b]
Dispersion (S22)	**0.16**[d]	**0.28**[b]	1.30[b]	1.50[b]	**0.40**[b]
Mixed (S22)	**0.23**[d]	0.61[b]	1.01[b]	1.01[b]	**0.50**[b]
S22 total	**0.27**[d]	**0.40**[b]	0.98[b]	1.00[b]	**0.38**[b]
Intramolecular Interactions					
ACONF	**0.07**[d]	0.19[b]	**0.12**[b]	0.23[b]	**0.07**[b]
CYCONF	**0.12**[d]	0.36[b]	0.68[b]	0.61[b]	0.42[b]
PCONF	**0.17**[d]	0.34[b]	0.69[b]	0.82[b]	**0.21**[b]
SCONF	**0.23**[d]	0.89[b]	**0.32**[b]	**0.37**[b]	**0.38**[b]

[a]CBS(4/3) extrapolated values. [b]Using the ATZ basis set. [c]Using the ATZ basis set and DFT-D3(BJ). [d]Taken from GMTKN30 database, using the def2-QZVP basis set and DFT-D3. [e]Using corrected atomic energies. [f]Taken from ref 69 using NL correction (b = 7.8). [g]The smallest MADs within 0.2 kcal mol^{-1} are shown in bold.

CONCLUSION

In this paper, we have developed a dual-hybrid method which is hybridized at two levels. First we calculate the self-consistent PBE0.75 reference orbitals yielded by a 0.75 fraction exact exchange containing PBE hybrid. Then we mix 0.75 fraction of exact exchange energy with 0.25 fraction of PBE exchange energy and add direct Random Phase Approximation, dRPA, correlation energy to obtain the dRPA75 energy. All energy components are calculated using the PBE0.75 hybrid reference orbitals. dRPA75 requires no extra computational effort compared to dRPA.

We used five reaction energies of small hydrocarbons, sHC5, and the six reaction barrier heights of the BH6 test set to analyze the dRPA hybridization errors. We have obtained extremely accurate and precise dRPA75 results even with the moderate augmented triple-ζ (ATZ) basis set for the reaction energies and barriers. Comparison to the best available methods for reaction energies (five homodesmotic reaction classes) and barriers (DBH24 and BH76 test sets) shows that dRPA75 is one of them, and it systematically improves the dRPA results. For Diels–Alder reactions (DARC) the dRPA75/ATZ leads to an average 2 kcal mol^{-1} endothermic reaction energy error with a good precision. The origin of this error is that the 0.25 fraction of the PBE exchange energy overcorrects the large exothermic error of the dRPA@PBE0.75/ATZ. Conventional DFT methods perform very poorly for the DARC test set.

The analysis of the binding energy curves of H_2^+ and H_2 yields that dRPA75 gives typical dRPA results for equilibrium bond distance and energy but shows large one-electron self-correlation error and a moderate static correlation error. The one-electron self-correlation error free RPAX2@PBEx yields perfect binding curve for H_2^+ and H_2. The beyond-RPA AXK removes most of the self-correlation of dRPA, but not all, and yields better description of static correlation than SOSEX.

DOI: 10.1021/acs.jctc.5b00420
J. Chem. Theory Comput. XXXX, XXX, XXX−XXX

The dRPA methods show typical serious underbinding errors, and the calculated atomization energies are very sensitive to the basis set. Even the A6Z basis set yields large but very systematic errors. The systematic underbinding and the basis set error can be corrected easily via corrected atomic energies. Contrarily, the imprecisions of the double hybrid methods (e.g., B2PLYP-D3) cannot be corrected as efficiently as the imprecisions of the dRPA methods.

For weak interactions in the NCCE31 test set, our results show that dRPA75 is much more accurate and precise for charge transfer interaction energies than the other dRPA methods and double hybrid functionals. dRPA75 also shows a very balanced performance for all categories of the test set, and it is considerably better than any of the methods discussed in this paper. For the S22 test set, dRPA75 performs quite well with slight overestimation of the interaction energies due to the basis set error. For intramolecular interactions in alkanes and peptides (ACONF, PCONF), dRPA75 shows excellent performance. It performs better than the other dRPA methods for cysteine and monosaccharide conformers (CYCONF, SCONF).

These results are quite promising. dRPA75 performs well in many areas of molecular physical chemistry and integrates seamlessly the noncovalent interactions. It shows all the strengths of the dRPA methods but performs better than dRPA@PBE or dRPA@PBE0.25. However, problems arise due to the self-interaction error of PBEx and dRPAc functionals. The elimination of these errors will be the topic of our future work.

■ ASSOCIATED CONTENT

Supporting Information

The Supporting Information is available free of charge on the ACS Publications website at DOI: 10.1021/acs.jctc.5b00420.

Further information about the parameter optimization, the complete basis set extrapolations, and detailed results with statistics (PDF)

■ AUTHOR INFORMATION

Corresponding Authors

*E-mail: mezei.pal@mail.bme.hu.

*E-mail: gcsonka@mail.bme.hu.

Notes

The authors declare no competing financial interest.

■ ACKNOWLEDGMENTS

This work was supported by the Department of Energy under Grant No. DE-SC0010499. The authors thank the Hungarian National higher education and research network for the computer time.

■ REFERENCES

(1) Langreth, D.; Perdew, J. P. *Phys. Rev. B* **1977**, *15*, 2884−2901.

(2) Langreth, D.; Perdew, J. P. *Phys. Rev. B: Condens. Matter Mater. Phys.* **1980**, *21*, 5469−5493.

(3) Yan, Z.; Perdew, J. P.; Kurth, S. *Phys. Rev. B: Condens. Matter Mater. Phys.* **2000**, *61*, 16430.

(4) Furche, F. *J. Chem. Phys.* **2008**, *129*, 114105.

(5) Kubo, R. *Rep. Prog. Phys.* **1966**, *29*, 255−284.

(6) Scuseria, G. E.; Henderson, T. M.; Sorensen, D. C. *J. Chem. Phys.* **2008**, *129*, 231101.

(7) Eshuis, H.; Bates, J. E.; Furche, F. *Theor. Chem. Acc.* **2012**, *131*, 1084.

(8) Eshuis, H.; Furche, F. *J. Phys. Chem. Lett.* **2011**, *2*, 983−989.

(9) Zhu, W.; Toulouse, J.; Savin, A.; Angyán, J. G. *J. Chem. Phys.* **2010**, *132*, 244108.

(10) Ren, X.; Rinke, P.; Scheffler, M. *Phys. Rev. B: Condens. Matter Mater. Phys.* **2009**, *80*, 1−8.

(11) Schimka, L.; Harl, J.; Stroppa, A.; Grüneis, A.; Marsman, M.; Mittendorfer, F.; Kresse, G. *Nat. Mater.* **2010**, *9*, 741−744.

(12) Lebègue, S.; Harl, J.; Gould, T.; Ángyán, J. G.; Kresse, G.; Dobson, J. F. *Phys. Rev. Lett.* **2010**, *105*, 196401.

(13) Harl, J.; Kresse, G. *Phys. Rev. B: Condens. Matter Mater. Phys.* **2008**, *77*, 1−8.

(14) Ruzsinszky, A.; Perdew, J. P.; Csonka, G. I. *J. Chem. Theory Comput.* **2010**, *6*, 127−134.

(15) Ruzsinszky, A.; Perdew, J. P.; Csonka, G. I. *J. Chem. Phys.* **2011**, *134*, 114110.

(16) Jiang, H.; Engel, E. *J. Chem. Phys.* **2007**, *127*, 184108.

(17) Furche, F. *Phys. Rev. B: Condens. Matter Mater. Phys.* **2001**, *64*, 195120.

(18) Harl, J.; Schimka, L.; Kresse, G. *Phys. Rev. B: Condens. Matter Mater. Phys.* **2010**, *81*, 115126.

(19) Ren, X.; Tkatchenko, A.; Rinke, P.; Scheffler, M. *Phys. Rev. Lett.* **2011**, *106*, 153003.

(20) Paier, J.; Ren, X.; Rinke, P.; Scuseria, G. E.; Grüneis, A.; Kresse, G.; Scheffler, M. *New J. Phys.* **2012**, *14*, 043002.

(21) Zhao, Y.; González-García, N.; Truhlar, D. G. *J. Phys. Chem. A* **2005**, *109*, 2012−2018.

(22) Grüneis, A.; Marsman, M.; Harl, J.; Schimka, L.; Kresse, G. *J. Chem. Phys.* **2009**, *131*, 154115.

(23) Paier, J.; Janesko, B. G.; Henderson, T. M.; Scuseria, G. E.; Grüneis, A.; Kresse, G. *J. Chem. Phys.* **2010**, *132*, 094103;Erratum: **2010**, *133*, 179902.

(24) Freeman, D. L. *Phys. Rev. B* **1977**, *15*, 5512−5521.

(25) Sai, N.; Barbara, P. F.; Leung, K. *Phys. Rev. Lett.* **2011**, *106*, 226403.

(26) Perdew, J. P.; Levy, M.; Balduz, J. L. *Phys. Rev. Lett.* **1982**, *49*, 1691−1694.

(27) Zhang, Y.; Yang, W. *Theor. Chem. Acc.* **2000**, *103*, 346−348.

(28) Yang, W.; Zhang, Y.; Ayers, P. *Phys. Rev. Lett.* **2000**, *84*, 5172.

(29) Perdew, J. P.; Ruzsinszky, A.; Csonka, G. I.; Vydrov, O.; Scuseria, G. E.; Staroverov, V. N.; Tao, J. *Phys. Rev. A: At., Mol., Opt. Phys.* **2007**, *76*, 040501(R).

(30) Atalla, V.; Yoon, M.; Caruso, F.; Rinke, P.; Scheffler, M. *Phys. Rev. B: Condens. Matter Mater. Phys.* **2013**, *88*, 165122.

(31) Levy, M.; Perdew, J. P.; Sahni, V. *Phys. Rev. A: At., Mol., Opt. Phys.* **1984**, *30*, 2745−2748.

(32) Macher, M.; Klimeš, J.; Franchini, C.; Kresse, G. *J. Chem. Phys.* **2014**, *140*, 084502.

(33) Heßelmann, A. *Phys. Rev. A: At., Mol., Opt. Phys.* **2012**, *85*, 012517.

(34) Bates, J. E.; Furche, F. *J. Chem. Phys.* **2013**, *139*, 171103.

(35) Grimme, S. *J. Chem. Phys.* **2006**, *124*, 034108.

(36) Kozuch, S.; Gruzman, D.; Martin, J. M. L. *J. Phys. Chem. C* **2010**, *114*, 20801−20808.

(37) Goerigk, L.; Grimme, S. *J. Chem. Theory Comput.* **2011**, *7*, 291−309.

(38) Kállay, M. *J. Chem. Phys.* **2014**, *141*, 244113.

(39) Csonka, G. I.; Kaminsky, J. *J. Chem. Theory Comput.* **2011**, *7*, 988−997.

(40) Mezei, P. D.; Csonka, G. I.; Ruzsinszky, A. *J. Chem. Theory Comput.* **2015**, *11*, 3961−3967.

(41) Mrcc, a quantum chemical program suite written by Kállay, M.; Rolik, Z.; Ladjánszki, I.; Szegedy, L.; Ladóczki, B.; Csontos, J.; Kornis, B. See also Rolik, Z.; Szegedy, L.; Ladjánszki, I.; Ladóczki, B.; Kállay, M. *J. Chem. Phys.* **2013**, *139*, 094105 as well as www.mrcc.hu10.1063/1.4819401.

(42) Neese, F. The ORCA program system. *Wiley Interdiscip. Rev.: Comput. Mol. Sci.* **2012**, *2*, 73−78.

(43) Pieniazek, S. N.; Clemente, F. R.; Houk, K. N. *Angew. Chem., Int. Ed.* **2008**, *47*, 7746−7749.

DOI: 10.1021/acs.jctc.5b00420
J. Chem. Theory Comput. XXXX, XXX, XXX−XXX

(44) NIST Computational Chemistry Comparison and Benchmark Database, NIST Standard Reference Database Number 101, Release 16a, August 2013, Johnson, R. D., III, Ed. http://cccbdb.nist.gov/ (accessed January 8, 2015).
(45) Wheeler, S. E.; Houk, K. N.; Schleyer, P. V. R.; Allen, W. D. *J. Am. Chem. Soc.* **2009**, *131*, 2547−2560.
(46) Johnson, E. R.; Mori-Sanchez, P.; Cohen, A. J.; Yang, W. *J. Chem. Phys.* **2008**, *129*, 204112.
(47) Mezei, P. D.; Csonka, G. I.; Kállay, M. *J. Chem. Theory Comput.* **2015**, *11*, 2879−2888.
(48) Lynch, B. J.; Truhlar, D. G. *J. Phys. Chem. A* **2003**, *107*, 8996−8999.
(49) Lynch, B. J.; Truhlar, D. G. *J. Phys. Chem. A* **2003**, *107*, 3898−3906.
(50) Haunschild, R.; Klopper, W. *Theor. Chem. Acc.* **2012**, *131*, 1112.
(51) Karton, A.; Tarnopolsky, A.; Lamère, J.-F.; Schatz, G. C.; Martin, J. M. L. *J. Phys. Chem. A* **2008**, *112*, 12868−12886.
(52) Zhao, Y.; Truhlar, D. G. *J. Chem. Theory Comput.* **2005**, *1*, 415−432.
(53) Zhao, Y.; Truhlar, D. G. *J. Phys. Chem. A* **2005**, *109*, 5656−5667.
(54) Jurecka, P.; Sponer, J.; Cerny, J.; Hobza, P. *Phys. Chem. Chem. Phys.* **2006**, *8*, 1985−1993.
(55) Takatani, T.; Hohenstein, E. G.; Malagoli, M.; Marshall, M. S.; Sherrill, C. D. *J. Chem. Phys.* **2010**, *132*, 144104.
(56) Gruzman, D.; Karton, A.; Martin, J. M. L. *J. Phys. Chem. A* **2009**, *113*, 11974−11983.
(57) Wilke, J. J.; Lind, M. C.; Schaefer, H. F., III; Csaszar, A. G.; Allen, W. D. *J. Chem. Theory Comput.* **2009**, *5*, 1511−1523.
(58) Reha, D.; Valdes, H.; Vondrasek, J.; Hobza, P.; Abu-Riziq, A.; Crews, B.; de Vries, M. S. *Chem. - Eur. J.* **2005**, *11*, 6803−6817.
(59) Csonka, G. I.; French, A. D.; Johnson, G. P.; Stortz, C. A. *J. Chem. Theory Comput.* **2009**, *5*, 679−692.
(60) Ruzsinszky, A.; Perdew, J. P.; Csonka, G. I.; Vydrov, O. A.; Scuseria, G. E. *J. Chem. Phys.* **2006**, *125*, 194112.
(61) Cohen, A. J.; Mori-Sánchez, P.; Yang, W. *Science* **2008**, *321*, 792−794.
(62) Goerigk, L.; Grimme, S. *Phys. Chem. Chem. Phys.* **2011**, *13*, 6670−6688.
(63) Mussard, B.; Reinhardt, P.; Ángyán, J. G.; Toulouse, J. *J. Chem. Phys.* **2015**, *142*, 154123.
(64) Perdew, J. P.; Sun, J.; Ruzsinszky, A.; Mezei, P. D.; Csonka, G. I. *Period. Polytech. Chem. Eng.* **2015**, DOI: 10.3311/PPch.8356.
(65) Csonka, G. I.; Ruzsinszky, A.; Tao, J.; Perdew, J. P. *Int. J. Quantum Chem.* **2005**, *101*, 506−511.
(66) Janesko, B. G.; Scuseria, G. E. *J. Chem. Phys.* **2008**, *128*, 244112.
(67) Dahlke, E. E.; Truhlar, D. G. *J. Phys. Chem. B* **2005**, *109*, 15677−15683.
(68) Eshuis, H.; Furche, F. *J. Chem. Phys.* **2012**, *136*, 084105.
(69) Aragó, J.; Ortí, E.; Sancho-García, J. C. *J. Chem. Theory Comput.* **2013**, *9*, 3437−3443.

DOI: 10.1021/acs.jctc.5b00420
J. Chem. Theory Comput. XXXX, XXX, XXX−XXX